

Supplementary material for: Interface-induced superconductivity and strain-dependent spin density waves in FeSe/SrTiO₃ thin films

Shiyong Tan,^{1,2} Yan Zhang,¹ Miao Xia,¹ Zirong Ye,¹ Fei Chen,¹ Xin Xie,¹ Rui Peng,¹ Difei Xu,¹ Qin Fan,¹ Haichao Xu,¹ Juan Jiang,¹ Tong Zhang,¹ Xinchun Lai,² Tao Xiang,³ Jiangping Hu,³ Binping Xie,¹ and Donglai Feng^{1,*}

¹*State Key Laboratory of Surface Physics, Department of Physics, and Advanced Materials Laboratory, Fudan University, Shanghai 200433, People's Republic of China*

²*China Academy of Engineering Physics, Mianyang, 621900, Sichuan, People's Republic of China*

³*Institute of Physics, Chinese Academy of Sciences, Beijing 100190, People's Republic of China*

Abstract

In this supplementary material, we present thickness dependence of the Brillouin zone size (Fig. S1), the band structures and superconducting properties of 1 ML and 2 ML FeSe films (Fig. S2), temperature broadening simulation of the electronic structure for the 50 ML FeSe film (Fig. S3) in detail. We also present electronic structure evidence for the spin density wave (SDW) order in multi-layer FeSe films with more than one monolayer (ML) thickness. The temperature dependence of the electronic structure around $(-\pi, 0)$ for 3 ML, 13 ML, 15 ML, 25 ML and 35 ML FeSe films are presented in Figs. S4-S8 respectively.

*Electronic address: dl.feng@fudan.edu.cn

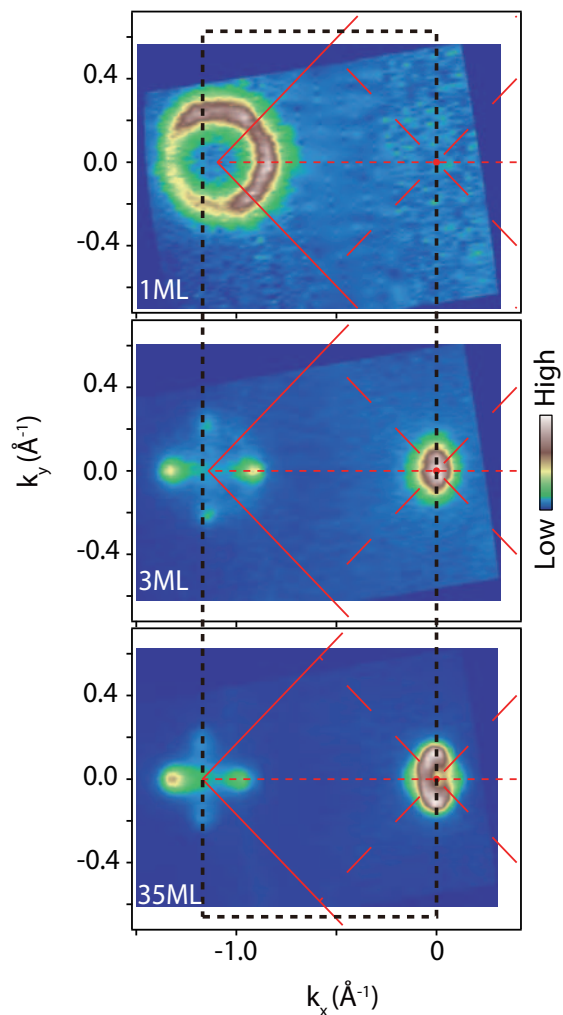


FIG. S1: **Thickness dependence of the Brillouin zone size.** The Fermi surface maps as represented by the photoemission intensity at the Fermi energy for 1 ML, 3 ML and 35 ML FeSe films at 30 K. The intensity was integrated over a window of $(E_F-10 \text{ meV}, E_F+10 \text{ meV})$. The Brillouin zone size increases with increased film thickness, and thus the lattice constant decreases with increased film thickness.

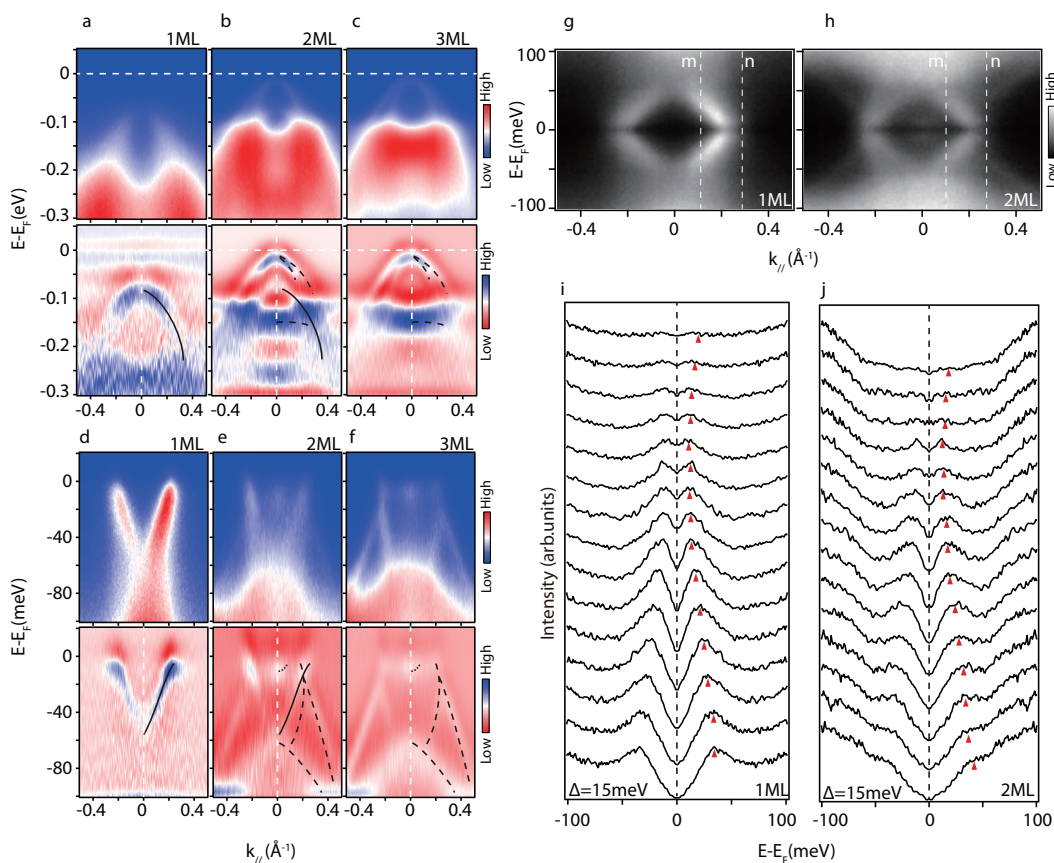


FIG. S2: The band structures and the superconducting properties of 1 ML and 2 ML FeSe films. **a, b** and **c**, The photoemission intensity and the corresponding second derivative with respect to energy around $(0, 0)$ for 1 ML, 2 ML and 3 ML FeSe films at 30K. The band structure is determined from the second derivative of the photoemission data with respect to energy. The solid lines correspond to the band structure of the interface FeSe layer, while the dashed lines correspond to the band structure of the surface FeSe layer of the multi-layer FeSe films. The band structure of 2 ML FeSe near $(0, 0)$ is a superposition of these two structures. **d, e** and **f**, The photoemission intensity and the corresponding second derivative with respect to energy around $(-\pi, 0)$ for 1 ML, 2 ML and 3 ML FeSe films at 30K. The measured band structure of 2 ML FeSe near $(-\pi, 0)$ is a superposition of those measured on single layer and multi-layer films. **g** and **h**, The symmetrized (with respect to E_F) photoemission intensity around $(-\pi, 0)$ for 1 ML and 2 ML FeSe films at 25K. The strong suppression of the spectral weight near E_F indicates the superconducting behavior in both films. **i** and **j**, The symmetrized EDCs integrated over cut m and cut n for 1 ML and 2 ML FeSe films, respectively. The sizes of the superconducting gap are the same for both 1 ML and 2 ML films.

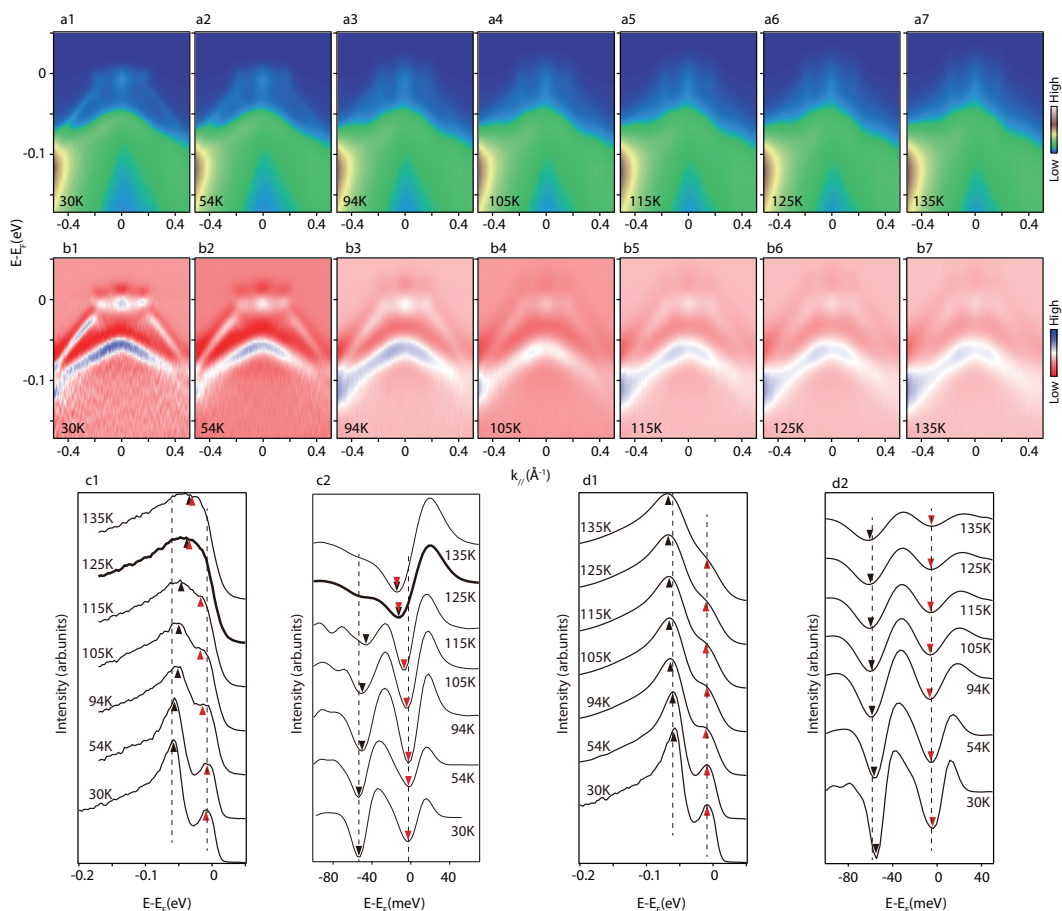


FIG. S3: Temperature broadening simulation of the electronic structure for the 50 ML FeSe film. a, The photoemission intensity near $(-\pi, 0)$ taken at 30 K (a1) and simulated intensity at higher temperatures (a2-a7). The high temperature data are obtained by convolve the 30K data with a Gaussian, which has a FWHM (full width at half maximum) of $3.5k_B T$ (k_B is the Boltzmann constant, and T is the corresponding temperature). **b,** The corresponding second derivative with respect to energy of data in panels **a1-a7**. **c,** The temperature dependence of (c1) the original experimental EDCs at $(-\pi, 0)$, and (c2) the corresponding second derivative with respect to energy. They show two separated bands merge into one above 125K. **d,** The temperature dependence of (d1) the simulated EDCs at $(-\pi, 0)$, and (d2) the corresponding second derivative with respect to energy. The two peaks (dips) gradually become broader with increasing temperature but do not merge into one. Therefore, the temperature broadening of the bands can not reproduce the observed remarkable temperature dependence of the electronic structure.

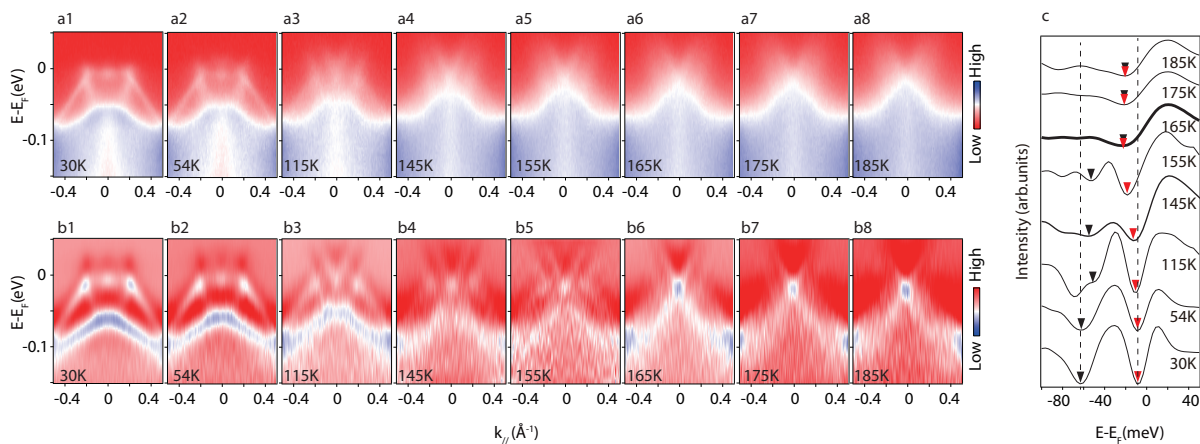


FIG. S4: **Temperature dependence of the electronic structure of the 3 ML FeSe film.** **a** and **b**, Temperature dependence of (a1-a8) the photoemission intensity around $(-\pi, 0)$, and (b1-b8) the corresponding second derivative with respect to energy. The two separated bands gradually merge into one above 165 K. **c**, The temperature dependence of the second derivative of the spectrum taken at $(-\pi, 0)$. T_A is determined to be 165 K based on the merging of the two marked dips.

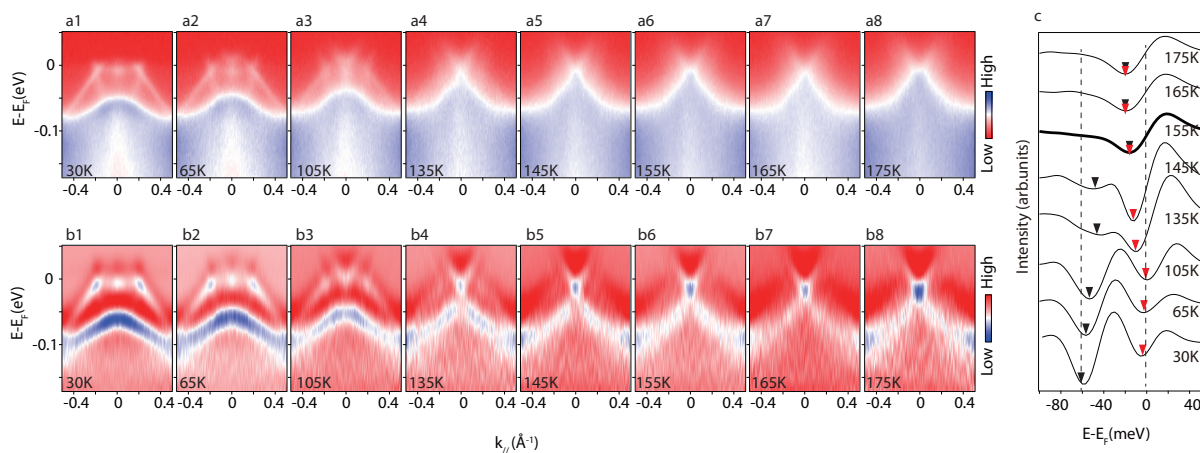


FIG. S5: **Temperature dependence of the electronic structure of the 13 ML FeSe film.** **a** and **b**, Temperature dependence of (a1-a8) the photoemission intensity around $(-\pi, 0)$, and (b1-b8) the corresponding second derivative with respect to energy. The two separated bands gradually merge into one above 155 K. **c**, The temperature dependence of the second derivative of the spectrum taken at $(-\pi, 0)$. T_A is determined to be 155 K based on the merging of the two marked dips.

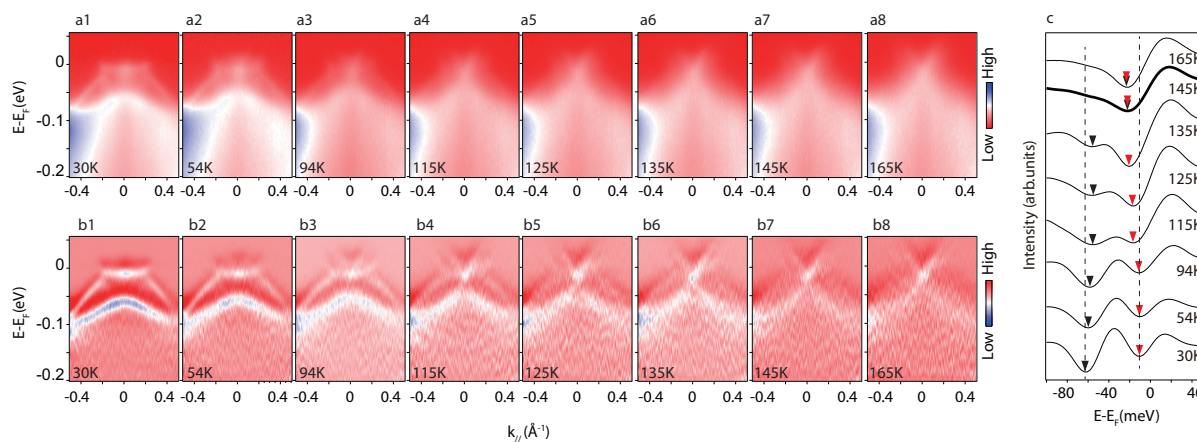


FIG. S6: Temperature dependence of the electronic structure of the 15 ML FeSe film. **a** and **b**, Temperature dependence of (a1-a8) the photoemission intensity around $(-\pi, 0)$, and (b1-b8) the corresponding second derivative with respect to energy. The two separated bands gradually merge into one above 145 K. **c**, The temperature dependence of the second derivative of the spectrum taken at $(-\pi, 0)$. T_A is determined to be 145 K based on the merging of the two marked dips.

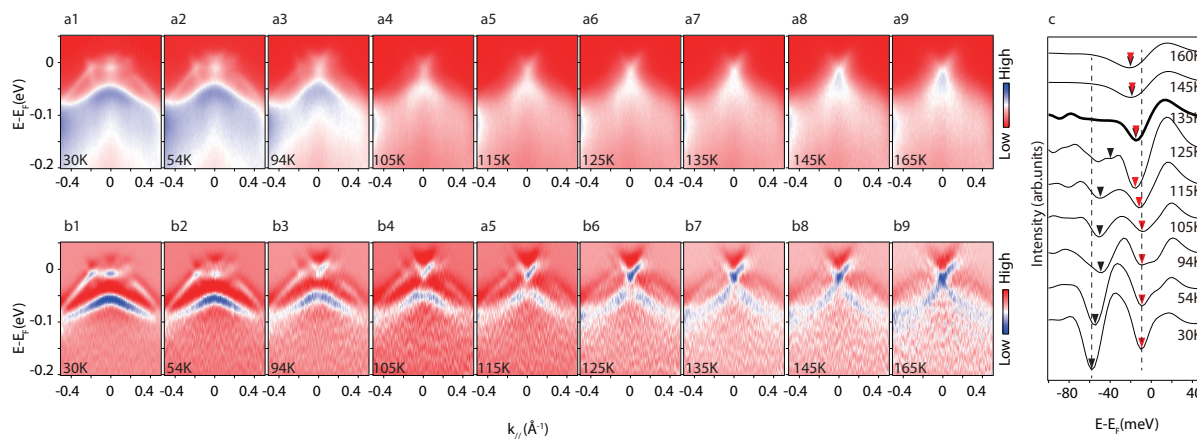


FIG. S7: Temperature dependence of the electronic structure of the 25 ML FeSe film. **a** and **b**, Temperature dependence of (a1-a9) the photoemission intensity around $(-\pi, 0)$, and (b1-b9) the corresponding second derivative with respect to energy. The two separated bands gradually merge into one above 135 K. **c**, The temperature dependence of the second derivative of the spectrum taken at $(-\pi, 0)$. T_A is determined to be 135 K based on the merging of the two marked dips.

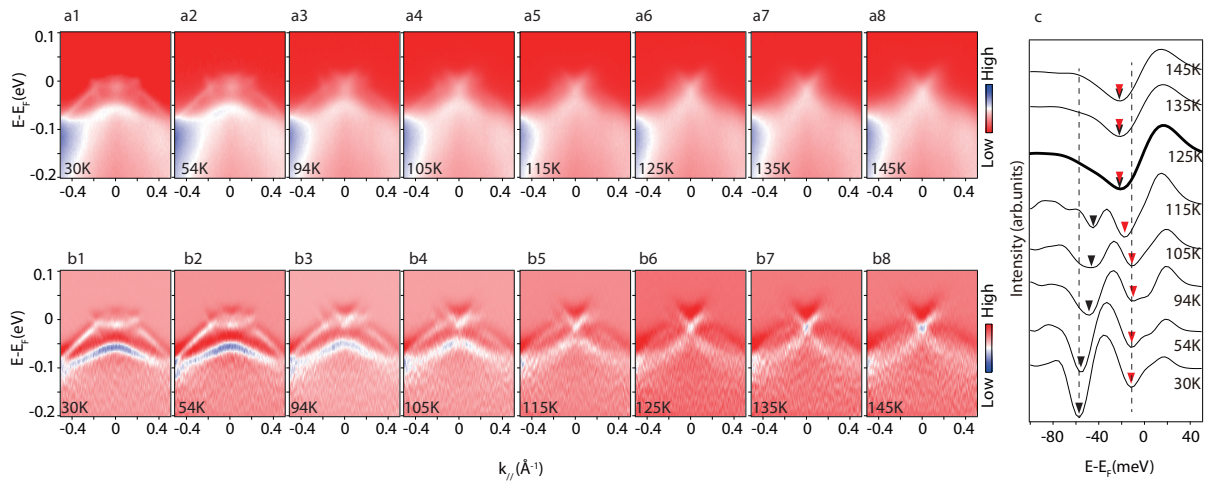


FIG. S8: Temperature dependence of the electronic structure of the 35 ML FeSe film. **a** and **b**, Temperature dependence of (a1-a8) the photoemission intensity around $(-\pi, 0)$, and (b1-b8) the corresponding second derivative with respect to energy. The two separated bands gradually merge into one above 125 K. **c**, The temperature dependence of the second derivative of the spectrum taken at $(-\pi, 0)$. T_A is determined to be 125 K based on the merging of the two marked dips.